

## Synergy between glutamate modulation and anti-programmed cell death protein 1 immunotherapy for glioblastoma

Ravi Medikonda, MD,<sup>1</sup> John Choi, MD,<sup>1</sup> Ayush Pant, BS,<sup>1</sup> Laura Saleh, BS,<sup>1</sup> Denis Routkovich, BS,<sup>1</sup> Luqing Tong, MD, PhD,<sup>1</sup> Zineb Belcaid, MD,<sup>1</sup> Young Hoon Kim, MD,<sup>2</sup> Christopher M. Jackson, MD,<sup>1</sup> Christina Jackson, MD,<sup>1</sup> Dimitrios Mathios, MD,<sup>1</sup> Yuanxuan Xia, MD,<sup>1</sup> Pavan P. Shah, BS,<sup>1</sup> Kisha Patel, BS,<sup>1</sup> Timothy Kim, BS,<sup>1</sup> Siddhartha Srivastava, BS,<sup>1</sup> Sakibul Huq, MD,<sup>1</sup> Jeff Ehresman, MD,<sup>1</sup> Zach Pennington, MD,<sup>1</sup> Betty Tyler, BA,<sup>1</sup> Henry Brem, MD,<sup>1</sup> and Michael Lim, MD<sup>1</sup>

<sup>1</sup>Department of Neurosurgery, The Johns Hopkins University School of Medicine, Baltimore, Maryland; and <sup>2</sup>Department of Neurosurgery, Asan Medical Center, University of Ulsan College of Medicine, Seoul, South Korea

**OBJECTIVE** Immune checkpoint inhibitors such as anti-programmed cell death protein 1 (anti-PD-1) have shown promise for the treatment of cancers such as melanoma, but results for glioblastoma (GBM) have been disappointing thus far. It has been suggested that GBM has multiple mechanisms of immunosuppression, indicating a need for combinatorial treatment strategies. It is well understood that GBM increases glutamate in the tumor microenvironment (TME); however, the significance of this is not well understood. The authors posit that glutamate upregulation in the GBM TME is immunosuppressive. The authors utilized a novel glutamate modulator, BHV-4157, to determine synergy between glutamate modulation and the well-established anti-PD-1 immunotherapy for GBM.

**METHODS** C57BL/6J mice were intracranially implanted with luciferase-tagged GL261 glioma cells. Mice were randomly assigned to the control, anti-PD-1, BHV-4157, or combination anti-PD-1 plus BHV-4157 treatment arms, and median overall survival was assessed. In vivo microdialysis was performed at the tumor site with administration of BHV-4157. Intratumoral immune cell populations were characterized with immunofluorescence and flow cytometry.

**RESULTS** The BHV-4157 treatment arm demonstrated improved survival compared with the control arm ( $p < 0.0001$ ). Microdialysis demonstrated that glutamate concentration in TME significantly decreased after BHV-4157 administration. Immunofluorescence and flow cytometry demonstrated increased CD4+ T cells and decreased Foxp3+ T cells in mice that received BHV-4157 treatment. No survival benefit was observed when CD4+ or CD8+ T cells were depleted in mice prior to BHV-4157 administration ( $p < 0.05$ ).

**CONCLUSIONS** In this study, the authors showed synergy between anti-PD-1 immunotherapy and glutamate modulation. The authors provide a possible mechanism for this synergistic benefit by showing that BHV-4157 relies on CD4+ and CD8+ T cells. This study sheds light on the role of excess glutamate in GBM and provides a basis for further exploring combinatorial approaches for the treatment of this disease.

<https://thejns.org/doi/abs/10.3171/2021.1.JNS202482>

**KEYWORDS** glioblastoma immunotherapy; glutamate modulation; anti-PD-1; oncology

**G**LIOMA (GBM) is the most aggressive primary malignant brain tumor.<sup>1</sup> Even with resection, radiation therapy, and chemotherapy, median overall survival is approximately 15 months for patients with GBM.<sup>2</sup> Over the past 10 years, median survival has changed little despite advancements in the understanding of the genomics and pathophysiology of GBM.<sup>1</sup> Howev-

er, these advancements have helped us better understand GBM's multiple mechanisms of treatment resistance.

There is enormous interest in applying anti-programmed cell death protein 1 (anti-PD-1) therapy to the treatment of GBM given the dramatic success of this therapy for other solid tumors, including melanoma and non-small cell lung cancer.<sup>3–5</sup> However, preliminary results

**ABBREVIATIONS** anti-PD-1 = anti-programmed cell death protein 1; FBS = fetal bovine serum; GBM = glioblastoma; HBSS = Hank's Balanced Salt Solution; IACUC = Institutional Animal Care and Use Committee; IF = immunofluorescence; IFNγ = interferon gamma; IP = intraperitoneally; IVIS = in vivo imaging system; PBS = phosphate-buffered saline; TIL = tumor-infiltrating lymphocyte; TME = tumor microenvironment; Treg = regulatory T cell.

**SUBMITTED** June 25, 2020. **ACCEPTED** January 26, 2021.

**INCLUDE WHEN CITING** Published online August 13, 2021; DOI: 10.3171/2021.1.JNS202482.

from the CheckMate 143 phase III clinical trial suggest that anti-PD-1 therapy alone does not significantly improve median survival compared with the current standard of care.<sup>6</sup> The underwhelming response of GBM to anti-PD-1 monotherapy suggests that GBM may have multiple mechanisms of immunosuppression in addition to the PD-1 axis.<sup>7</sup> Other mechanisms of GBM immunoresistance include high tumor heterogeneity, immune cell sequestration in bone marrow, iatrogenic factors, and local cytokine release.<sup>8–11</sup> As a result of having numerous immunosuppressive mechanisms, GBM has been characterized as a “cold” tumor with a paucity of tumor-infiltrating lymphocytes (TILs) and an abundance of immunosuppressive myeloid cells.<sup>12</sup> A major focus of current research on immunotherapy for GBM is to further understand the immunosuppressive mechanisms of GBM through exploration of the many cell types and small molecules that constitute the tumor microenvironment (TME).<sup>3</sup>

Glutamate is a small molecule in the GBM TME that has been implicated in both GBM pathophysiology and immune system suppression. Two separate studies have demonstrated glutamate receptor-dependent functional synapses between neural cells and glioma cells.<sup>13,14</sup> Furthermore, synaptic activity between neurons and glioma cells is mediated by these glutamate receptors and promotes glioma proliferation. These studies highlight the important role that glutamate plays as a neurotransmitter in the growth of glial tumors. Furthermore, there is evidence that glutamate also significantly influences the immune system. Ganor and Levite concluded that low physiological glutamate concentration significantly improves T-cell function and survival; however, high pathologic glutamate concentration has an inhibitory effect on T-cell function.<sup>15</sup> Indeed, they reported that glutamate concentration in the range of  $10^{-3}$  to  $10^{-2}$  M significantly inhibited activated T-cell proliferation.<sup>15</sup> Furthermore, Chiocchetti et al. showed that human T cells exposed to glutamate concentrations between  $10^{-8}$  and  $10^{-4}$  M were significantly protected from activation-induced cell death.<sup>16</sup> Given that GBM upregulates glutamate in the TME,<sup>17</sup> we hypothesized that a potential mechanism of GBM immunosuppression is that the pathologically elevated glutamate concentration in the TME inhibits TIL function.

Because glutamate impacts both the immune system and glioma progression,<sup>13–15</sup> we aimed to study glutamate modulation with the novel drug BHV-4157, a prodrug formulation of riluzole, as an immunotherapy strategy for GBM. BHV-4157 is currently under investigation in clinical trials for Alzheimer’s disease (ClinicalTrials.gov identifier NCT03605667), spinocerebellar ataxia (NCT02960893), and obsessive compulsive disorder (NCT03299166). It has been proposed that BHV-4157 facilitates increased reuptake of glutamate from the synaptic terminal. We used a murine GBM model to show that BHV-4157 reduces the glutamate concentration in the GBM TME and synergizes with anti-PD-1 immune checkpoint therapy.

## Methods

### Mice

Six- to 8-week-old wild-type C57BL/6J female mice

(Jackson Laboratories) were housed at the Johns Hopkins University Animal Facility. All animal experiments were conducted in accordance with the protocols approved by the Johns Hopkins Institutional Animal Care and Use Committee (IACUC).

### Cell Lines

Luciferase-tagged GL261 (GL261-Luc+) (RRID: CVCL\_X986) cells were maintained in Dulbecco’s Modified Eagle Medium (Gibco) with 10% fetal bovine serum (FBS) (Sigma-Aldrich) and 1% penicillin-streptomycin (Sigma-Aldrich). This GL261-Luc+ cell line was provided by the Reardon Lab (Dana-Farber Cancer Institute). Cells were cultured in a 37°C incubator with 5% CO<sub>2</sub>. All experiments were performed using mycoplasma-free cells.

### Intracranial Murine Glioma Model

In total, 130,000 GL261-Luc+ cells were stereotactically injected into the left cortical hemisphere, as previously described.<sup>19</sup> Tumor presence was confirmed with a bioluminescent *in vivo* imaging system (IVIS) on day 7 after tumor implantation. All mice with a high-intensity signal on IVIS were confirmed to have tumor and randomly assigned to the treatment arms for each experiment.

### Drugs

BHV-4157 was obtained from Biohaven Pharmaceuticals. Anti-PD-1 was obtained from hamster anti-murine PD-1 monoclonal antibody-producing hybridoma (G4), as previously described.<sup>20</sup> We administered intraperitoneally (IP) 15 mg/kg/day BHV-4157 beginning on day 8 after tumor confirmation with bioluminescent IVIS. This dosing schedule was established on the basis of the results of pilot studies on dose escalation and toxicity. We administered IP 10 mg/kg anti-PD-1 on days 10, 12, and 14 after tumor implantation.

### Survival Analysis

Survival experiments were performed in duplicate with at least 8 mice per treatment arm. The following treatment arms were included: control, BHV-4157, anti-PD-1, and BHV-4157 plus anti-PD-1. Mice were euthanized when they became moribund or developed severe neurological deficits based on the criteria established by our IACUC. IVIS results obtained on day 7 after implantation are provided in Supplemental Fig. 1.

### Microdialysis

Tumor-bearing mice were anesthetized using an isoflurane vaporizer (Kent Scientific), which provided a standardized gas concentration to each mouse via the outlet tube. We used 2.5% isoflurane and 1.25% isoflurane to induce and maintain anesthesia, respectively. The oxygen flow rate was kept at 1.0 L/min throughout the experiment. After induction of anesthesia, a CMA 7 guide cannula (Harvard Apparatus) was implanted into the brain using the previous burr hole created for tumor implantation. A CMA 7 microdialysis probe (Harvard Apparatus) was then inserted via the guide cannula. The inlet tube of

the microdialysis probe was connected to a microinfusion pump (World Precision Instruments), and the outlet tube was connected to a 200- $\mu$ l polymerase chain reaction tube for collection of dialysate. The microinfusion pump was used to perfuse the microdialysis probe with artificial cerebrospinal fluid (Harvard Apparatus) at a rate of 1.0  $\mu$ l/min. A 2-hour equilibrium period was used before collection of samples. Thereafter, samples were collected every 30 minutes and immediately frozen at -20°C.

The first hour of sample collection occurred before treatment administration (time point -1 to 0 hours) and represents baseline glutamate concentration. Then, BHV-4157 or phosphate-buffered saline (PBS), as a control solution, was administered IP 2 hours after the start of sample collection. Samples were collected for an additional 4 hours after treatment administration. The Glutamate-Glo assay (Promega) was utilized to measure the glutamate concentration in each collected dialysate sample. The manufacturer's protocol for this assay was used to measure the glutamate concentration in each dialysate sample. Data are presented as the percentage of the baseline glutamate concentration.

### Depletion Studies

Tumor-bearing mice received IP injections of either 200  $\mu$ g/dose anti-CD4 (clone GK1.5, Bio X Cell) or 500  $\mu$ g/dose anti-CD8 (clone 2.43, Bio X Cell). Control mice received IP 200  $\mu$ l of PBS. Antibodies were administered 48 and 24 hours before the first dose of BHV-4157, and then readministered every 7 days thereafter for 3 weeks. Pretreatment cell depletion was confirmed with flow cytometric analysis of peripheral blood immune cells on day 10 after tumor implantation.

### Immunofluorescence Staining

Five mice per treatment arm were intracranially implanted with GL261 tumor cells and treated, as described above. The following treatment arms were included: control, BHV-4157, anti-PD-1, and BHV-4157 plus anti-PD-1. Mice were euthanized on day 18 after tumor implantation, and each mouse brain was snap frozen. Each brain was sectioned to 5- $\mu$ m intervals with a cryostat. Immunofluorescence (IF) staining was performed using primary antibodies CD4 (clone 4SM95), CD8 (clone 4SM16), and vimentin (clone EPR3776). Secondary antibody fluorophores were Alexa Fluor 488 and Alexa Fluor 594. All primary and secondary antibodies were obtained from Thermo Fisher. All slides were counterstained with nuclear stain DAPI. Additionally, the first slide from each brain was stained with hematoxylin and eosin to confirm tumor presence. Images were obtained of randomly selected microscopic fields of the intratumoral niche in each brain.

### Immune Cell Isolation

To isolate splenocytes, spleens were harvested from mice on day 18 after implantation. Whole solid organs were mechanically homogenized in RPMI medium with 10% FBS and 1% penicillin-streptomycin and filtered through a 70- $\mu$ m mesh cell strainer (BD Falcon). Red blood cells were lysed (ACK Lysing Buffer, Quality Biological), and

the remaining cells were washed with PBS. To isolate TILs, brains were harvested, mechanically homogenized, and filtered through a 70- $\mu$ m filter on day 18 after implantation. Each sample was resuspended in 5 ml of 72% Percoll in 1x Hank's Balanced Salt Solution (HBSS) (Gibco) without phenol red, layered below 5 ml of 36% Percoll Plus (GE Healthcare) in 1x HBSS, and centrifuged at 2000 rotations per minute for 20 minutes at room temperature. The cell layer at the interface between the 36% and 72% Percoll layers was collected and washed with PBS.

### Flow Cytometry and Immunophenotyping

Immune cells were isolated from the spleen and brain of each mouse and plated in a 96-well plate. For interferon gamma (IFN $\gamma$ ) staining, cells were first stimulated for 4 hours at 37°C in RPMI with 5000 $\times$  phorbol myristate acetate and 1500 $\times$  ionomycin prior to flow cytometric staining. Lymphocytes were stained for live/dead Aqua, CD3, CD45, CD4, CD8, Ki-67, Foxp3, PD-1, TIM-3, and LAG-3. For analysis of intracellular markers Ki-67, IFN $\gamma$ , and Foxp3, cells were fixed in a fixation/permeabilization mixture (Invitrogen) for 30 minutes and then stained with Ki-67, IFN $\gamma$ , and Foxp3 in permeabilization buffer (Invitrogen). See Supplemental Table 1 for the fluorophore conjugates and antibody concentrations used for each antibody. All samples were processed using a BD FACSCelesta flow cytometer (BD Biosciences). Data were analyzed using FlowJo version 10.2 (FlowJo, LLC). The gating strategy is presented in Supplemental Fig. 2.

### Statistical Analysis

Survival was analyzed with Kaplan-Meier survival curves, and these curves were compared with the log-rank Mantel-Cox test. One-way ANOVA was used to determine significance among multiple groups. The unpaired t-test was used to compare two groups. For the Glutamate-Glo assay, all samples were run in triplicate and the median value of each time point was used in final analysis. The baseline glutamate concentration was calculated as the mean of the last three consecutive samples obtained immediately prior to treatment. Subsequently, change in glutamate concentration over time was calculated as the percentage of the baseline glutamate concentration for each individual animal. Microdialysis data were analyzed with 2-factor ANOVA followed by Fisher's least significant difference test for multiple comparisons. All data were analyzed using Prism 8 (GraphPad). Statistical significance was defined as  $p < 0.05$ .

## Results

### BHV-4157 Conferred a Survival Benefit and Synergized With Anti-PD-1 Immunotherapy

A survival study was conducted with glioma-bearing mice to determine whether BHV-4157 has an antitumor effect and whether this drug could synergize with anti-PD-1 therapy. The four treatment arms were control, BHV-4157 alone, anti-PD-1 alone, and anti-PD-1 plus BHV-4157 (Fig. 1 upper). Eight to 10 mice were included in each treatment arm. The median survival was 22 days for the control arm, 30 days for the BHV-4157 mono-

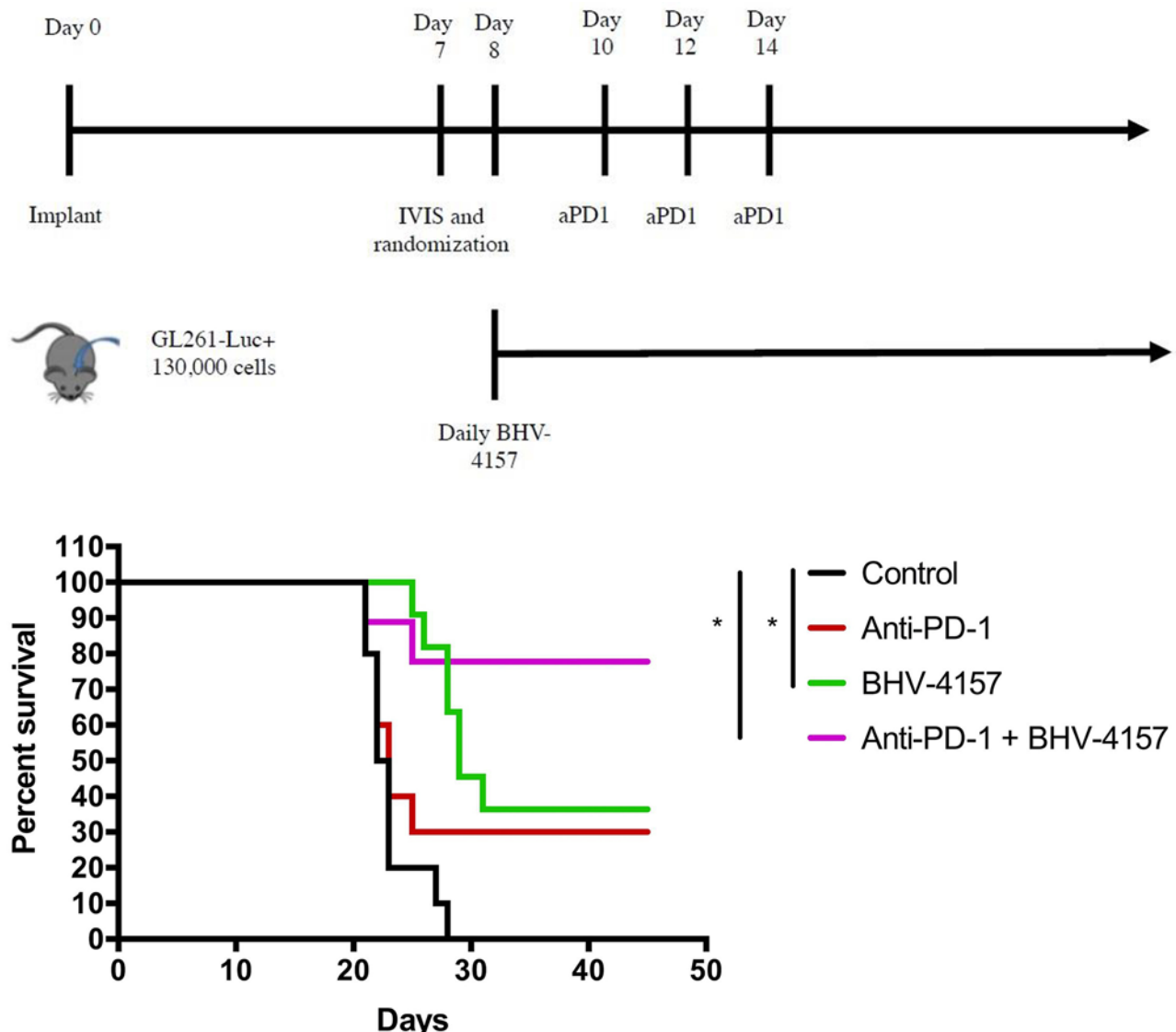


**FIG. 1.** Survival experiment. **Upper:** Schema of the experiment and treatment schedule. GL261-Luc+ cells were implanted on day 0. IVIS was performed on day 7. Mice with confirmed tumor on IVIS were randomly assigned to the experimental treatment arms. BHV-4157 was administered daily starting on day 8. Anti-PD-1 (aPD1) was administered on days 10, 12, and 14. **Lower:** Kaplan-Meier survival curve. The asterisks indicate statistical significance ( $p < 0.05$ ):  $p < 0.0001$  for the comparison of the BHV-4157 treatment arm ( $n = 11$ ) with the control arm ( $n = 10$ ); and  $p = 0.0007$  for the comparison of the combination treatment arm ( $n = 10$ ) with the control arm. Overall survival of the combination treatment arm was 80%, compared with 36% for the BHV-4157-only arm, 30% for anti-PD-1-only arm ( $n = 10$ ), and 0% for the control arm. Survival analysis was performed using the log-rank Mantel-Cox test. Figure is available in color online only.

therapy arm, and 23 days for the anti-PD-1 monotherapy arm (Fig. 1 lower); the median overall survival of the anti-PD-1 plus BHV-4157 combination therapy arm could not be determined because overall survival was 80%. The BHV-4157 treatment arm demonstrated significantly improved median survival compared with the control arm ( $p < 0.0001$ ). The anti-PD-1 treatment arm did not demonstrate significantly improved median survival compared with the control arm, but overall survival at 45 days was 30% for this arm compared with 0% for the control arm. The overall 45-day survival rates of the BHV-4157 monotherapy and combination therapy arms were 36% and

80%, respectively. The BHV-4157 plus anti-PD-1 treatment arm demonstrated significantly improved overall survival compared with the control arm ( $p = 0.0007$ ) and had more long-term surviving mice than either monotherapy arm (Fig. 1 lower).

#### BHV-4157 Decreased Glutamate in the Glioma TME

After demonstrating that BHV-4157 improved overall survival and synergized with anti-PD-1 therapy, we aimed to characterize the mechanism of the survival benefit of BHV-4157. BHV-4157 has been described as a CNS glutamate modulator,<sup>18</sup> so we used *in vivo* microdialysis to

study how BHV-4157 treatment alters glutamate concentration in the TME. Microdialysis was performed on 4 control mice that were administered PBS and 4 treated mice that were administered BHV-4157. After we administered IP BHV-4157 at time point 0, glutamate concentration in the treated mice began to decrease after 30 minutes and was significantly lower than the glutamate concentration of the control mice at 1 hour after treatment. The glutamate concentration of the BHV-4157 treatment arm decreased by approximately 50% of the pretreatment baseline value, but there was no significant change in the glutamate concentration of the control arm (Fig. 2). The glutamate concentration of the BHV-4157 treatment arm remained significantly lower than that of the control arm at the end of microdialysis recording, which was 4 hours after administration of treatment.

### BHV-4157 Decreased Regulatory T Cells and Increased Non-Regulatory T-Cell Proliferation in Glioma TME

Because T cells have glutamate receptors and can respond to changes in glutamate concentration,<sup>15,21</sup> we explored whether decreased glutamate concentration in TME after treatment with BHV-4157 affects immune cell infiltration of the tumor. IF staining was performed on 5 mice per treatment arm, including the control, anti-PD-1 only, BHV-4157 only, and combination therapy arms. IF staining showed increased CD4+ T-cell infiltration, but not CD8+ T-cell infiltration, in the tumors of mice treated with BHV compared with those of mice in the control or anti-PD-1 treatment arms. The combination BHV-4157 plus anti-PD-1 arm showed increased CD4+ and CD8+ T-cell infiltration compared with the control arm (Fig. 3).

Flow cytometric analysis was performed on 5–6 mice per treatment arm to quantify differences in immune cell populations between treatment arms and to further characterize our IF observations. Mice treated with BHV-4157 plus anti-PD-1 had a lower percentage of intratumoral CD4+Foxp3+ regulatory T cells (Tregs) than control mice ( $p = 0.0135$ ). We also saw a trend toward decreased CD4+Foxp3+ Treg cells in mice that received BHV-4157 treatment alone compared with control mice ( $p = 0.07$ ; Fig. 4A). Next, mice treated with BHV-4157 had a greater percentage of cells positive for the proliferation marker Ki-67 on CD3+ T cells than control mice ( $p = 0.0031$ ). Likewise, there was a similar increase in the percentage of Ki-67+CD3+ T cells in mice treated with combination therapy compared with that of control mice ( $p = 0.004$ ). Furthermore, the percentage of Ki-67+CD3+ T cells was significantly greater in mice treated with BHV-4157 monotherapy ( $p = 0.0426$ ) or combination therapy ( $p = 0.0240$ ) than in mice treated with anti-PD-1 therapy alone (Fig. 4B).

Next, we looked specifically at CD4+Foxp3− non-Treg cells (Fig. 4C). We found no differences in Ki-67 expression on CD4+Foxp3− cells among the control, BHV-4157 monotherapy, and anti-PD-1 monotherapy arms. However, we found significantly increased Ki-67 expression levels on CD4+Foxp3− cells in the combination arm compared with the control or either monotherapy arm ( $p = 0.02$ ,  $p = 0.01$ , and  $p = 0.01$ , respectively). We evaluated IFNγ expression in CD4+Foxp3− non-Treg TILs and found that BHV monotherapy and combination therapy significantly

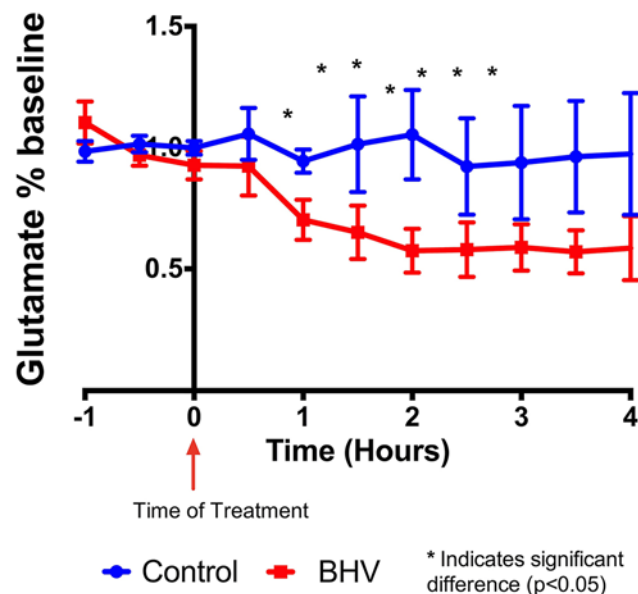


**FIG. 2.** In vivo microdialysis analysis in mice. The baseline glutamate concentration was established during the 1st hour of dialysate collection prior to treatment administration (time points −1 hour to 0 hour). Then, BHV-4157 ( $n = 4$ ) or PBS as a control ( $n = 4$ ) was injected IP at the 0-hour time point. The asterisks indicate statistical significance ( $p < 0.05$ ) for the comparison of the BHV-4157 arm with the control arm at the indicated time point. BHV-4157 treatment led to a significant decrease in intratumoral glutamate within 1 hour, and this effect persisted for at least an additional 3 hours. Statistical analysis was performed with 2-factor ANOVA followed by Fisher's least significant difference test. Dots and squares indicate mean values, and error bars indicate standard deviation. Figure is available in color online only.

increased IFNγ expression in CD4+Foxp3− TILs compared with IFNγ expression in the control ( $p = 0.03$  for BHV monotherapy vs control, and  $p = 0.002$  for combination therapy vs control) or anti-PD-1 monotherapy ( $p = 0.02$  for BHV monotherapy vs anti-PD-1 monotherapy, and  $p = 0.003$  for combination therapy vs anti-PD-1 monotherapy) treatment arms (Fig. 4D).

We also evaluated Ki-67 expression on CD8+ T cells (Fig. 4E). We found that Ki-67 expression on CD8+ T cells was not significantly different among the control, BHV-4157 monotherapy, and anti-PD-1 monotherapy arms, but Ki-67 expression was significantly greater in the control arm than the BHV-4157 monotherapy arm ( $p = 0.02$ ) and combination therapy arm ( $p = 0.01$ ).

Finally, we evaluated markers of exhaustion—PD-1, TIM-3, and LAG-3—on CD4+ and CD8+ T cells in the four treatment arms. Specifically, we evaluated the percentages of CD4+ and CD8+ T cells that expressed all three markers of exhaustion. The four treatment arms had similar percentages of CD8+ T cells that expressed all three markers of exhaustion (Fig. 4F). However, mice treated with combination therapy had a significantly lower percentage of CD4+ T cells that expressed all three markers of exhaustion than mice in the control ( $p = 0.02$ ), BHV-4157 only ( $p = 0.03$ ), or anti-PD-1 only ( $p = 0.03$ ) treatment arms (Fig. 4G).

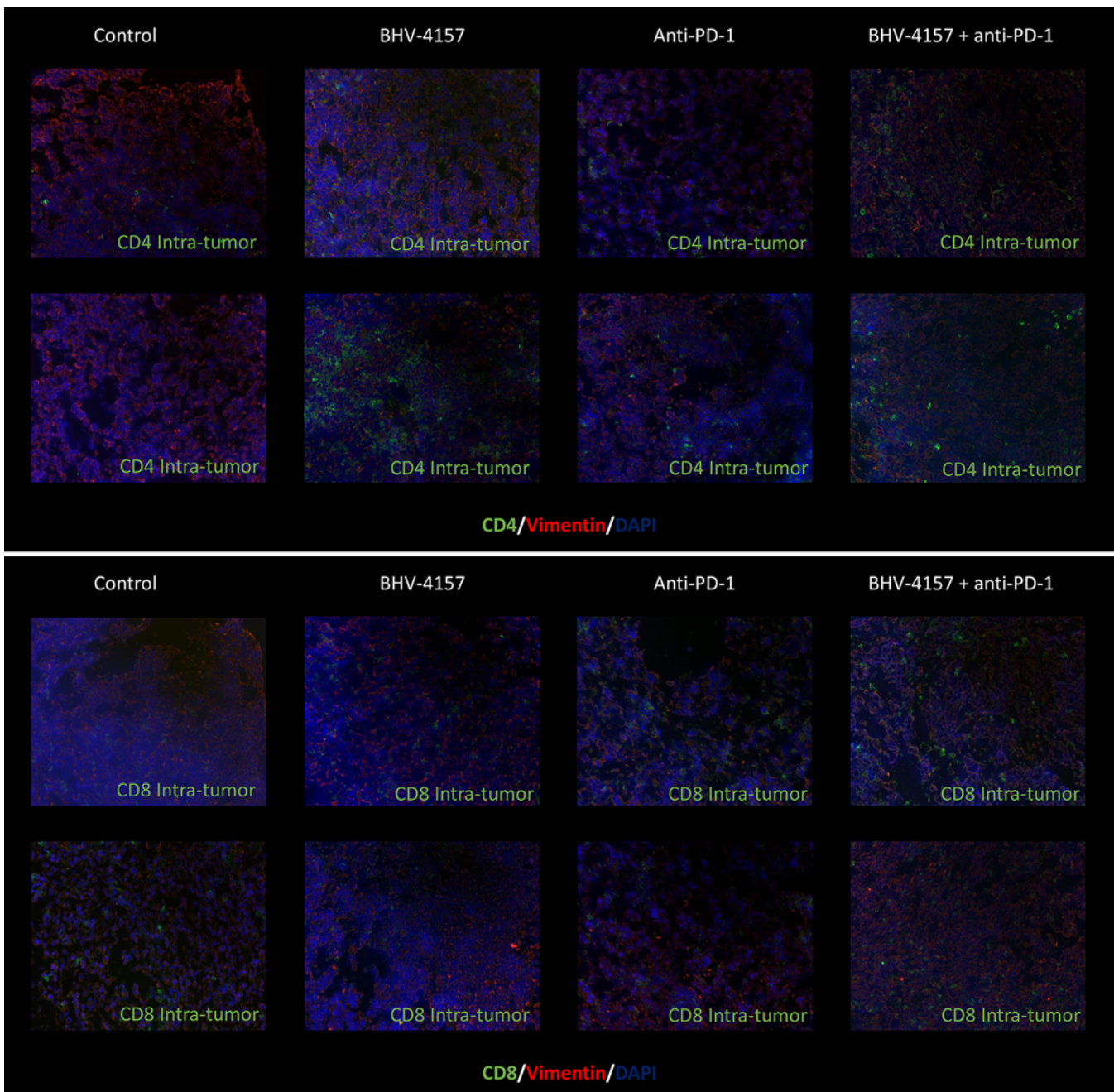


**FIG. 3.** Representative intratumoral IF images (magnification  $\times 20$ ). Two microscopic fields are presented for each stain. **Upper:** CD4+ staining of all four treatment arms. **Lower:** CD8+ staining of all four treatment arms. CD4+ and CD8+ staining is presented in green, vimentin in red, and DAPI in dark blue. The BHV-4157 treatment arm showed increased IF staining of the CD4+ T cells within the tumor compared with the control or anti-PD-1 arms. The anti-PD-1 treatment arm demonstrated increased IF staining of CD8+ T cells compared with the control or BHV-4157 treatment arms. Figure is available in color online only.

### CD4+ and CD8+ T Cells Are Necessary for BHV-4157 to Confer a Survival Advantage

After finding that BHV-4157 affected TILs, we explored whether CD4+ and CD8+ T cells were necessary for BHV-4157 to confer a survival advantage to glioma-bearing mice (Fig. 5). We utilized 8–10 mice per treatment arm in this depletion study. We depleted either CD4+ T

cells or CD8+ T cells prior to BHV-4157 treatment. We confirmed depletion of these T cells with flow cytometric analysis of blood samples on day 10 after implantation (Supplemental Fig. 3). Median overall survival was 23 days for the control arm, the treatment arm that underwent CD4+ T-cell depletion prior to BHV-4157 administration, and the treatment arm that underwent CD8+ T-cell depletion prior to BHV-4157 administration. The treatment arm

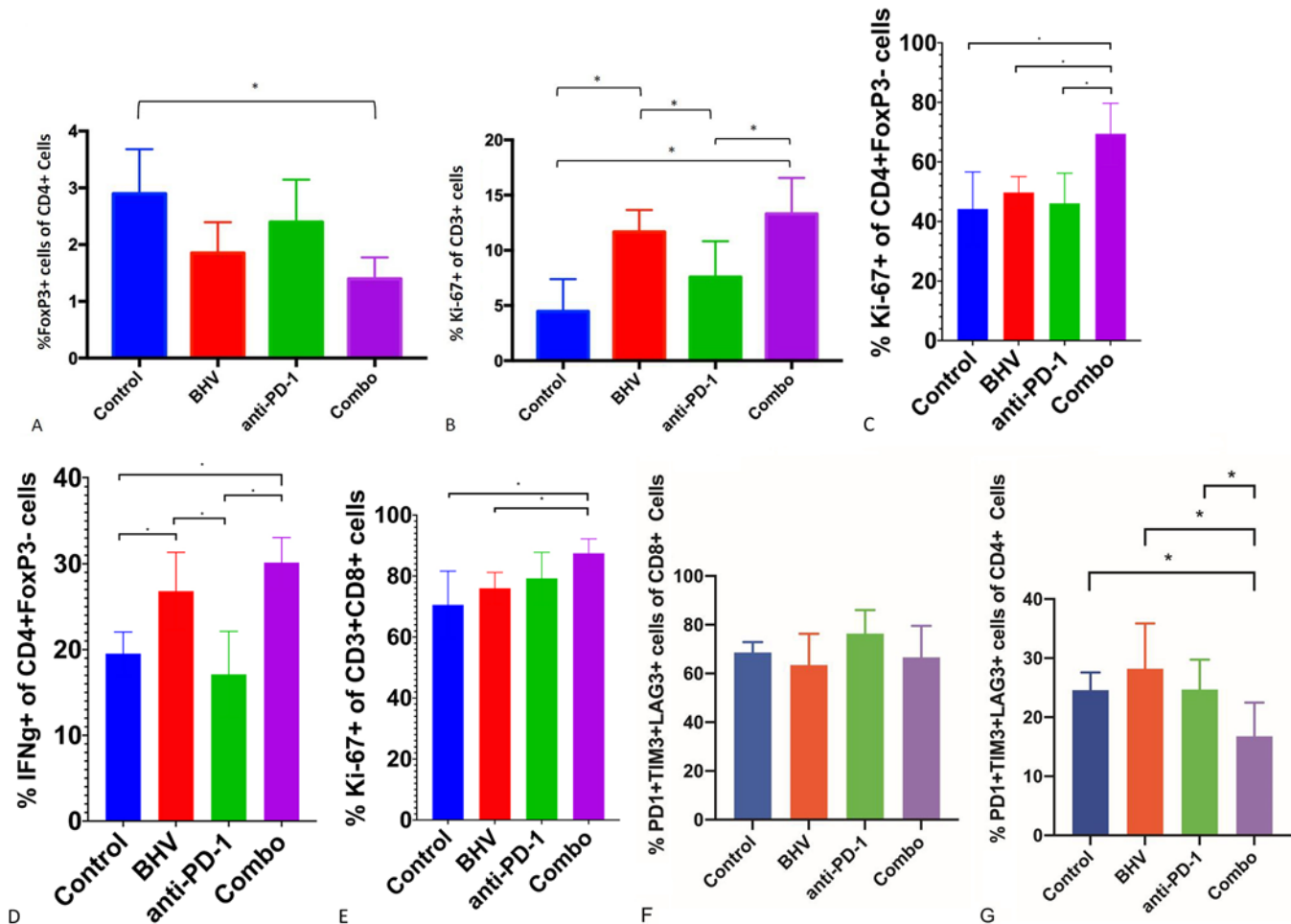


**FIG. 4.** Results of flow cytometric analysis of immune cell populations in the brains of tumor-bearing mice (5 mice per treatment arm). **A:** Mice treated with combination therapy had a lower percentage of CD4+Foxp3+ Treg cells in the brain compared with mice in the control arm ( $p = 0.0135$ ). **B:** The percentage of CD3+Ki-67+ cells in the brain was higher in the BHV-4157 treatment arm ( $p = 0.0031$ ) or combination therapy arm ( $p = 0.004$ ) compared with that of the control arm. Additionally, the percentage of CD3+Ki-67+ cells in the brain was higher in the BHV-4157 treatment arm ( $p = 0.0426$ ) or combination therapy arm ( $p = 0.0240$ ) compared with that of the anti-PD-1 arm. **C:** Ki-67 expression on CD4+Foxp3- TILs was significantly higher in the combination therapy arm than the control ( $p = 0.02$ ), BHV monotherapy ( $p = 0.01$ ), or anti-PD-1 monotherapy ( $p = 0.01$ ) arms. **D:** BHV monotherapy increased IFN $\gamma$  (IFNg) expression in CD4+Foxp3- TILs compared with IFNg expression in the control ( $p = 0.03$ ) or anti-PD-1 monotherapy ( $p = 0.02$ ) arms. IFNg expression was increased in CD4+Foxp3- TILs in the combination therapy arm compared with that of the control ( $p = 0.002$ ) or anti-PD-1 monotherapy ( $p = 0.003$ ) arms. **E:** Ki-67 expression was significantly higher on CD8+ TILs in the combination therapy arm than those of the control ( $p = 0.02$ ) or BHV monotherapy ( $p = 0.01$ ) arms. **F:** Percentages of CD8+ T cells that expressed all three markers of exhaustion (PD-1, TIM-3, and LAG-3) were similar among the four treatment arms. **G:** The combination treatment arm had a significantly smaller percentage of CD4+ T cells that expressed all three markers of exhaustion (PD-1, TIM-3, and LAG-3) than the control ( $p = 0.02$ ), BHV-4157 only ( $p = 0.03$ ), or anti-PD-1 only ( $p = 0.03$ ) treatment arms. Bars indicate mean values, and error bars indicate standard deviation. \* $p < 0.05$ . Figure is available in color online only.

that received BHV-4157 without T-cell depletion had a median overall survival of 27 days, which was significantly greater than that of the control ( $p = 0.04$ ), CD4+ T-cell depletion ( $p = 0.01$ ), and CD8+ T-cell depletion ( $p = 0.02$ ) treatment arms (Fig. 5).

## Discussion

Immunotherapy has garnered interest as a treatment of GBM given its success in other solid tumors, but clinical trials have failed to show a survival benefit for anti-PD-1

therapy compared with the standard of care for GBM.<sup>22</sup> This lack of response suggests that the highly immunosuppressive GBM TME contributes to the difficulty treating this disease. Therefore, it may be prudent to employ a combinatorial treatment strategy to target multiple distinct immunosuppressive mechanisms when treating GBM. Our study demonstrated that BHV-4157 is a potent modulator of glutamate in the glioma TME and confers a survival advantage in the GL261 murine glioma model. We have shown that BHV-4157 treatment induced a survival benefit, promoted proliferation of tumor-infiltrating

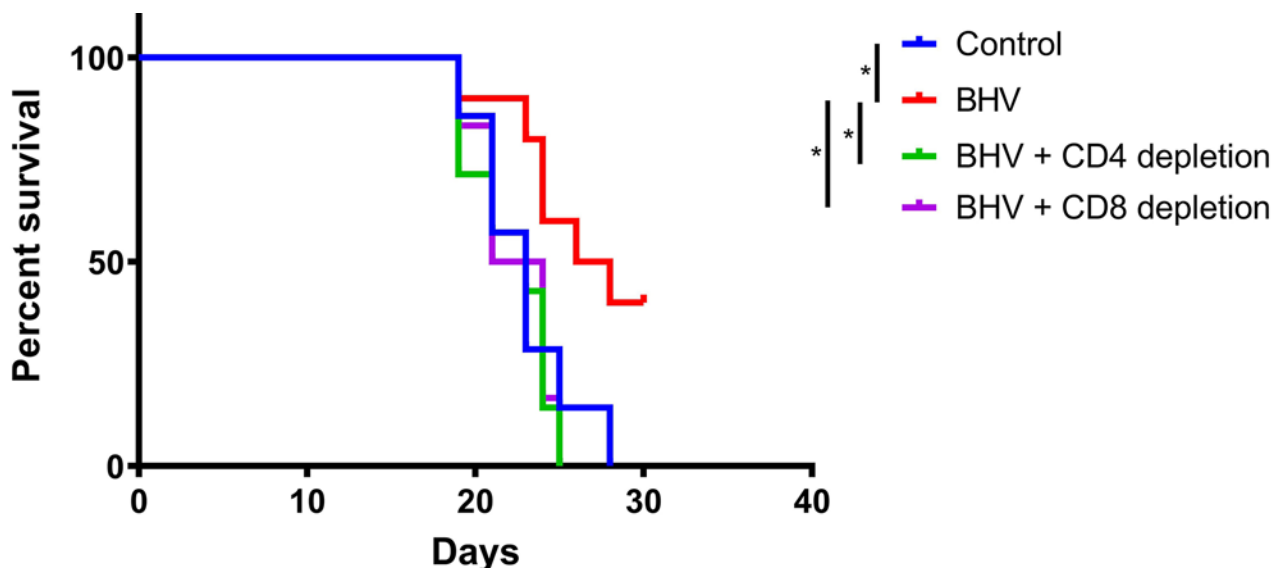


**FIG. 5.** Depletion survival study. Mice were depleted of either CD4+ T cells or CD8+ T cells prior to treatment with BHV-4157. There were no differences in survival among the control arm, CD4+ T-cell depletion plus BHV-4157 arm, and the CD8+ T-cell depletion plus BHV-4157 arm. The BHV-4157-only arm, without any depletion, had significantly improved survival compared with the control ( $p = 0.04$ ), BHV-4157 plus CD4+ T-cell depletion ( $p = 0.01$ ), and BHV-4157 plus CD8+ T-cell depletion ( $p = 0.02$ ) arms. \* $p < 0.05$ . Figure is available in color online only.

T cells, and synergized with anti-PD-1 immunotherapy to further improve survival and reduce Treg cells in the glioma TME.

GBM actively secretes glutamate, and this small molecule is found in abundance within the GBM TME.<sup>23,24</sup> Gliomas that secrete more glutamate have been shown to have a growth advantage in rodent models.<sup>25</sup> Furthermore, glutamate has been shown to play an important role in GBM invasion.<sup>26</sup> It has been suggested that the glutamate released by GBM is excitotoxic to healthy neurons, leading to cell death and providing the tumor with potential space for growth. All these studies suggest that glutamate has an integral role in the pathophysiology of GBM. We posited that increased glutamate in the TME may also play a role in immunosuppression by GBM, because several studies have suggested that immune cells have glutamate receptors and respond to changes in glutamate concentration.<sup>27–30</sup> Ganor and Levite found that physiological glutamate concentrations in the nanomolar and micromolar range can activate many vital T-cell functions, including migration, adhesion, and proliferation. However, increased glutamate concentration in the millimolar range can be pathologic and suppress key T-cell functions.<sup>15</sup> Thus, we hypothesized that excessive glutamate in the GBM TME may inhibit immune cell function and that BHV-4157 could reverse this process by decreasing glutamate in the TME.

Our IF data suggest that there was increased concentration of CD4+ T cells in TME after BHV-4157 treatment. To further characterize the subtype and activation status of the CD4+ T cells observed on IF staining, we conducted flow cytometric analysis. This allowed us to confirm that combination therapy led to decreased CD4+Foxp3+ Treg cells in the TME. Furthermore, we found that BHV-4157

monotherapy and combination therapy led to increased CD3+ TIL proliferation. More specifically, the combination therapy arm demonstrated increased proliferation of CD4+Foxp3– non-Treg TILs compared with the control or monotherapy arms. Both the BHV monotherapy and combination therapy arms demonstrated increased IFN $\gamma$  expression on CD4+FoxP3– non-Treg TILs compared with the control arm, but only combination therapy increased both proliferation and IFN $\gamma$  expression on CD4+Foxp3– non-Treg TILs. Furthermore, combination therapy increased CD8+ TIL proliferation to a greater extent than control or BHV monotherapy. Combination therapy also decreased the percentage of CD4+ T cells that expressed all three markers of exhaustion, PD-1, TIM-3, and LAG-3. The findings of the depletion study suggest that both CD4+ and CD8+ T cells are necessary for BHV-4157 to improve glioma survival. All together, these results suggest that there is increased tumor infiltration, proliferation, and activity of CD4+Foxp3– non-Treg TILs after treatment with combination therapy. We posit that increased CD4+Foxp3– T-cell proliferation and tumor infiltration enhance CD8+ T-cell antitumor activity. This is consistent with studies in the literature that have reported that CD4+ helper T cells play an important role in enabling the antitumor response of CD8+ effector T cells.<sup>31,32</sup>

The synergy between BHV-4157 and anti-PD-1 therapy suggests that BHV-4157 may target a different mechanism of immunosuppression than anti-PD-1 therapy. The PD-1/PD-L1 axis has been studied in GBM, and inhibition of this axis via anti-PD-1 therapy has been shown to improve CD8+ T-cell antitumor function.<sup>33</sup> We found that BHV-4157 primarily affected T cells, especially CD4+ T cells. Thus, the combination treatment of BHV-4157

and anti-PD-1 may simultaneously activate both non-Treg CD4+ T cells and effector CD8+ T cells, leading to a more robust antitumor immune response than either therapy alone.

A significant consideration of any preclinical study of GBM is the translatability of the results of a preclinical animal model to human patients with GBM. In this study, we used GL261 cells from a stable, syngeneic cell line culture, with the primary advantages being that they are well characterized and can be orthotopically implanted into immunocompetent C57BL/6J mice.<sup>34</sup> Furthermore, GL261 recapitulates many of the characteristics of GBM, including histological features such as pseudo-palisading necrosis and clinical features such as lack of metastasis and lack of spontaneous regression, which is a common issue with several murine glioma models.<sup>35</sup> A disadvantage of the GL261 model of GBM is that the significant heterogeneity in human GBM is not fully recapitulated in this animal model. Additionally, GL261 is a moderately immunogenic tumor model, whereas GBM is known to have significant immune resistance.<sup>22</sup> Nevertheless, GL261 is one of the most frequently used murine brain tumor models, and it is perhaps the most extensively used model for preclinical studies of immunotherapy for GBM.<sup>35,36</sup> For greater generalizability, additional experiments should be conducted with other GBM cell lines.

## Conclusions

This study highlights the importance of using combinatorial treatment strategies to overcome the immunosuppressive nature of GBM. Our results shed light on an additional immunosuppressive role of excessive glutamate in the GBM TME and provide a basis for further exploration of combinatorial approaches to GBM therapy. We believe that effective treatment of GBM will require the activation of multiple immune system compartments that work together to generate a strong antitumor response.

## References

- Ostrom QT, Gittleman H, Liao P, et al. CBTRUS Statistical Report: primary brain and other central nervous system tumors diagnosed in the United States in 2010-2014. *Neuro Oncol.* 2017;19(suppl 5):v1–v88.
- Stupp R, Mason WP, van den Bent MJ, et al. Radiotherapy plus concomitant and adjuvant temozolomide for glioblastoma. *N Engl J Med.* 2005;352(10):987–996.
- McGranahan T, Therkelsen KE, Ahmad S, Nagpal S. Current state of immunotherapy for treatment of glioblastoma. *Curr Treat Options Oncol.* 2019;20(3):24.
- Weber JS, D'Angelo SP, Minor D, et al. Nivolumab versus chemotherapy in patients with advanced melanoma who progressed after anti-CTLA-4 treatment (CheckMate 037): a randomised, controlled, open-label, phase 3 trial. *Lancet Oncol.* 2015;16(4):375–384.
- Paz-Ares L, Luft A, Vicente D, et al. Pembrolizumab plus chemotherapy for squamous non-small-cell lung cancer. *N Engl J Med.* 2018;379(21):2040–2051.
- Omuro A, Vlahovic G, Lim M, et al. Nivolumab with or without ipilimumab in patients with recurrent glioblastoma: results from exploratory phase I cohorts of CheckMate 143. *Neuro Oncol.* 2018;20(5):674–686.
- Mathios D, Lim M. Why is immunotherapy for glioblastoma “Lag”-ging. *Oncotarget.* 2019;10(12):1228–1229.
- Chongsathidkiet P, Jackson C, Koyama S, et al. Sequestration of T cells in bone marrow in the setting of glioblastoma and other intracranial tumors. *Nat Med.* 2018;24(9):1459–1468.
- Mathios D, Kim JE, Mangraviti A, et al. Anti-PD-1 antitumor immunity is enhanced by local and abrogated by systemic chemotherapy in GBM. *Sci Transl Med.* 2016;8(370):370ra180.
- Kaminska B, Kocyk M, Kijewska M. TGF beta signaling and its role in glioma pathogenesis. *Adv Exp Med Biol.* 2013;986:171–187.
- Patel AP, Tirosh I, Trombetta JJ, et al. Single-cell RNA-seq highlights intratumoral heterogeneity in primary glioblastoma. *Science.* 2014;344(6190):1396–1401.
- Rutledge WC, Kong J, Gao J, et al. Tumor-infiltrating lymphocytes in glioblastoma are associated with specific genomic alterations and related to transcriptional class. *Clin Cancer Res.* 2013;19(18):4951–4960.
- Venkatesh HS, Morishita W, Geraghty AC, et al. Electrical and synaptic integration of glioma into neural circuits. *Nature.* 2019;573(7775):539–545.
- Venkataramani V, Taney DI, Strahle C, et al. Glutamatergic synaptic input to glioma cells drives brain tumour progression. *Nature.* 2019;573(7775):532–538.
- Ganor Y, Levite M. The neurotransmitter glutamate and human T cells: glutamate receptors and glutamate-induced direct and potent effects on normal human T cells, cancerous human leukemia and lymphoma T cells, and autoimmune human T cells. *J Neural Transm (Vienna).* 2014;121(8):983–1006.
- Chiocchetti A, Miglio G, Mesturini R, et al. Group I mGlu receptor stimulation inhibits activation-induced cell death of human T lymphocytes. *Br J Pharmacol.* 2006;148(6):760–768.
- Choi J, Stradmann-Bellinghausen B, Yakubov E, et al. Glioblastoma cells induce differential glutamatergic gene expressions in human tumor-associated microglia/macrophages and monocyte-derived macrophages. *Cancer Biol Ther.* 2015;16(8):1205–1213.
- Huang LK, Chao SP, Hu CJ. Clinical trials of new drugs for Alzheimer disease. *J Biomed Sci.* 2020;27(1):18.
- Zeng J, See AP, Phallen J, et al. Anti-PD-1 blockade and stereotactic radiation produce long-term survival in mice with intracranial gliomas. *Int J Radiat Oncol Biol Phys.* 2013;86(2):343–349.
- Hirano F, Kaneko K, Tamura H, et al. Blockade of B7-H1 and PD-1 by monoclonal antibodies potentiates cancer therapeutic immunity. *Cancer Res.* 2005;65(3):1089–1096.
- Shanker A, de Aquino MTP, Hodo T, Uzhachenko R. Glutamate receptors provide costimulatory signals to improve T cell immune response. *J Immunol.* 2018;200(1 Suppl):47.24.
- Lim M, Xia Y, Bettegowda C, Weller M. Current state of immunotherapy for glioblastoma. *Nat Rev Clin Oncol.* 2018;15(7):422–442.
- Ye ZC, Sontheimer H. Glioma cells release excitotoxic concentrations of glutamate. *Cancer Res.* 1999;59(17):4383–4391.
- Behrens PF, Langemann H, Strohschein R, et al. Extracellular glutamate and other metabolites in and around RG2 rat glioma: an intracerebral microdialysis study. *J Neurooncol.* 2000;47(1):11–22.
- Takano T, Lin JH, Arcuino G, et al. Glutamate release promotes growth of malignant gliomas. *Nat Med.* 2001;7(9):1010–1015.
- Lyons SA, Chung WJ, Weaver AK, et al. Autocrine glutamate signaling promotes glioma cell invasion. *Cancer Res.* 2007;67(19):9463–9471.
- Ganor Y, Besser M, Ben-Zakay N, et al. Human T cells express a functional ionotropic glutamate receptor GluR3, and glutamate by itself triggers integrin-mediated adhesion to laminin and fibronectin and chemotactic migration. *J Immunol.* 2003;170(8):4362–4372.

28. Mashkina AP, Tyulina OV, Solovyova TI, et al. The excitotoxic effect of NMDA on human lymphocyte immune function. *Neurochem Int*. 2007;51(6-7):356–360.
29. Pacheco R, Ciruela F, Casadó V, et al. Group I metabotropic glutamate receptors mediate a dual role of glutamate in T cell activation. *J Biol Chem*. 2004;279(32):33352–33358.
30. Lombardi G, Miglio G, Dianzani C, et al. Glutamate modulation of human lymphocyte growth: in vitro studies. *Biochem Biophys Res Commun*. 2004;318(2):496–502.
31. Pardoll DM, Topalian SL. The role of CD4+ T cell responses in antitumor immunity. *Curr Opin Immunol*. 1998;10(5):588–594.
32. Kalams SA, Walker BD. The critical need for CD4 help in maintaining effective cytotoxic T lymphocyte responses. *J Exp Med*. 1998;188(12):2199–2204.
33. Huang J, Liu F, Liu Z, et al. Immune checkpoint in glioblastoma: promising and challenging. *Front Pharmacol*. 2017;8:242.
34. Lenting K, Verhaak R, Ter Laan M, et al. Glioma: experimental models and reality. *Acta Neuropathol*. 2017;133(2):263–282.
35. Oh T, Fakurnejad S, Sayegh ET, et al. Immunocompetent murine models for the study of glioblastoma immunotherapy. *J Transl Med*. 2014;12:107.
36. Maes W, Van Gool SW. Experimental immunotherapy for malignant glioma: lessons from two decades of research in the GL261 model. *Cancer Immunol Immunother*. 2011;60(2):153–160.

## Disclosures

Dr. Lim receives research support from Arbor, BMS, Accuray, Tocagen, Biohaven, and Kyrin-Kyowa; is a consultant for Tocagen, VBI, InCephalo Therapeutics, Pyramid Bio, Merck, BMS, Insightec, Biohaven, Sanianoia, Hemispherian, Black Diamond Therapeutics, and Novocure; is a shareholder for Egret Therapeutics; has patents for Focused radiation plus checkpoint inhibitors, Local chemotherapy plus checkpoint inhibitors, and Checkpoints for Neuro-Inflammation; and is a non-research consultant for Stryker. Ms. Tyler holds a patent with Accelerating Combination Therapies. Dr. Brem is a consultant for Acuity Bio Corp., Accelerating Combination Therapies, Camden Partners, Like Minds Inc., Galen Robotics Inc., and Nurami Medical; and has a nonfinancial relationship with NIH, AsclepiX Therapeutics, StemGen, and InSightec. This project received funding support from Biohaven Pharmaceuticals, which manufactures BHV-4157.

Therapeutics, and Novocure; is a shareholder for Egret Therapeutics; has patents for Focused radiation plus checkpoint inhibitors, Local chemotherapy plus checkpoint inhibitors, and Checkpoints for Neuro-Inflammation; and is a non-research consultant for Stryker. Ms. Tyler holds a patent with Accelerating Combination Therapies. Dr. Brem is a consultant for Acuity Bio Corp., Accelerating Combination Therapies, Camden Partners, Like Minds Inc., Galen Robotics Inc., and Nurami Medical; and has a nonfinancial relationship with NIH, AsclepiX Therapeutics, StemGen, and InSightec. This project received funding support from Biohaven Pharmaceuticals, which manufactures BHV-4157.

## Author Contributions

Conception and design: Lim. Acquisition of data: Medikonda, Choi, Pant, Saleh, Routkevitch, Tong, Belcaid, YH Kim, Xia, Shah, Patel, T Kim, Srivastava, Huq, Ehresman, Pennington. Analysis and interpretation of data: Lim, Medikonda, Choi, Pant, Belcaid. Drafting the article: Lim, Medikonda. Critically revising the article: Lim, Medikonda, Choi, CM Jackson, C Jackson, Mathios, Tyler, Brem. Reviewed submitted version of manuscript: Lim, Medikonda. Approved the final version of the manuscript on behalf of all authors: Lim. Statistical analysis: Medikonda. Study supervision: Lim.

## Online-Only Content

Supplemental material is available with the online version of the article.

*Supplemental Table and Figures.* <https://thejns.org/doi/suppl/10.3171/2021.1.JNS202482>.

## Correspondence

Michael Lim: The Johns Hopkins University School of Medicine, Baltimore, MD. [mlim3@jhmi.edu](mailto:mlim3@jhmi.edu).